Materials and Structures/Matériaux et Constructions, 1988, **21**, 425/430

Size effect tests of torsional failure of plain and reinforced concrete beams

ZDENĚK P. BAŽANT, SIDDIK ŞENER,* PERE C. PRAT
Center for Concrete and Geomaterials, Northwestern University, Evanston, Illinois 60208, USA

The current design code formulae for the torsional failure of plain or longitudinally reinforced beams exhibit no size effect, i.e. the failure of geometrically similar beams of different sizes is supposed to occur at the same nominal stress. Experiments on reduced-scale beams were carried out, and the results confirm that there is a significant size effect, such that the nominal stress at failure decreases as the beam size increases. This is found for both plain and longitudinally reinforced beams. The results are consistent with the recently proposed Bažant's size-effect law. However, the scatter of the results and the scope and range limitations prevent it from being concluded that the applicability of this law is proven.

1. INTRODUCTION

The current design code formulae for torsional failure of plain as well as longitudinally reinforced concrete beams are based on plastic limit analysis [1]. This failure theory exhibits no size effect, i.e. geometrically similar specimens of different sizes are supposed to fail at the same nominal stress. Torsional failure, however, is brittle rather than plastic, as evidenced by the fact that the load does not attain a horizontal plateau but decreases after reaching a maximum value. For this reason the existence of a size effect should be expected.

Among the test data existing in the literature (reviewed by Bažant and Şener [2]), most give no information on the size effect. Those which do [3–6] were not designed with the checking of a possible size effect in mind. The size effects in these are obscured by other influences. Existence of the size effect can nevertheless be discerned in the existing data and its form is not inconsistent with Bažant's size-effect law [8].

2. TESTING METHOD AND RESULTS

The test specimens, shown in Figs 1 to 7, were square prisms of cross-section side d and length L. Three specimen sizes characterized by d = 38.1, 76.2 and 152.4 mm (1.5, 3 and 6 in.) were used, and the ratio L/d = 8/3 was the same for all beams. The beams were loaded by opposite couples at their ends as illustrated in Figs 1, 3, 6 and 7. The arms of the loading couples and beam ends were 19.1, 38.1 and 127 mm (0.75, 1.5 and 5 in.). The forces of the couples were applied at distance a from the beam end, such that a/L = 3/32 for all beams. The loads were applied through spherical bearings on steel bearing plates glued by epoxy to the concrete surface. The bearing plates, made of stainless steel, were square, of sizes 9.5, 19.1 and 38.1 mm (0.375, 0.75 and 1.5 in.), and the thickness of all the plates was 6.4 mm (0.25 in.). To avoid kinematic indeterminancy and at the same time prevent axial forces, one bearing was prevented from rolling in both directions and another one in the transverse direction only.

The specimens were made of microconcrete with maximum gravel size 4.8 mm (0.19 in.) and maximum sand size 3.35 mm (0.132 in.). The gravel consisted of crushed limestone, and the sand was a siliceous Illinois beach sand (Lake Michigan). The mix ratio cement:sand:gravel:water was 1:2:2:0.6. Portland cement C150 of ASTM Type I was used. The specimens were removed from their plywood moulds one day after casting and were then cured for three weeks in water. After that they were kept in a moist room at 24°C (75°F) temperature until the time of test. The age of the specimens at the time of test was 28 days. The specimens were cast from three different batches of concrete, two specimens of each size from each batch. Three companion cylinders of diameter 76.2 mm (3 in.) and length 152.4 mm (6 in.) were also cast from each batch. The uniaxial compression strengths of these cylinders after 28 days of curing are listed in Table 1.

Two types of specimen were tested: plain and reinforced. The reinforced specimens of the aforementioned three sizes contained four longitudinal bars placed in the cross-section corners with a cover of 8.1, 16.3 and 31.5 mm (0.32, 0.64 and 1.25 in.), respectively. Deformed bars of diameters 3.18, 6.35 and 12.7 mm (0.125, 0.25 and 0.5 in.) were used. For the smallest diameters, the yield strength was f_y = 310 MPa (45 000 psi), and for the larger ones it was f_y = 413 MPa (60 000 psi). To ensure proper load transmission, both the reinforced and plain specimens were provided with additional steel stirrups at the ends, as shown in Fig. 2. From each batch of concrete mixed, one specimen of each size as well as three control cylinders were cast. The

* On leave from Technical University, Istanbul, Turkey.

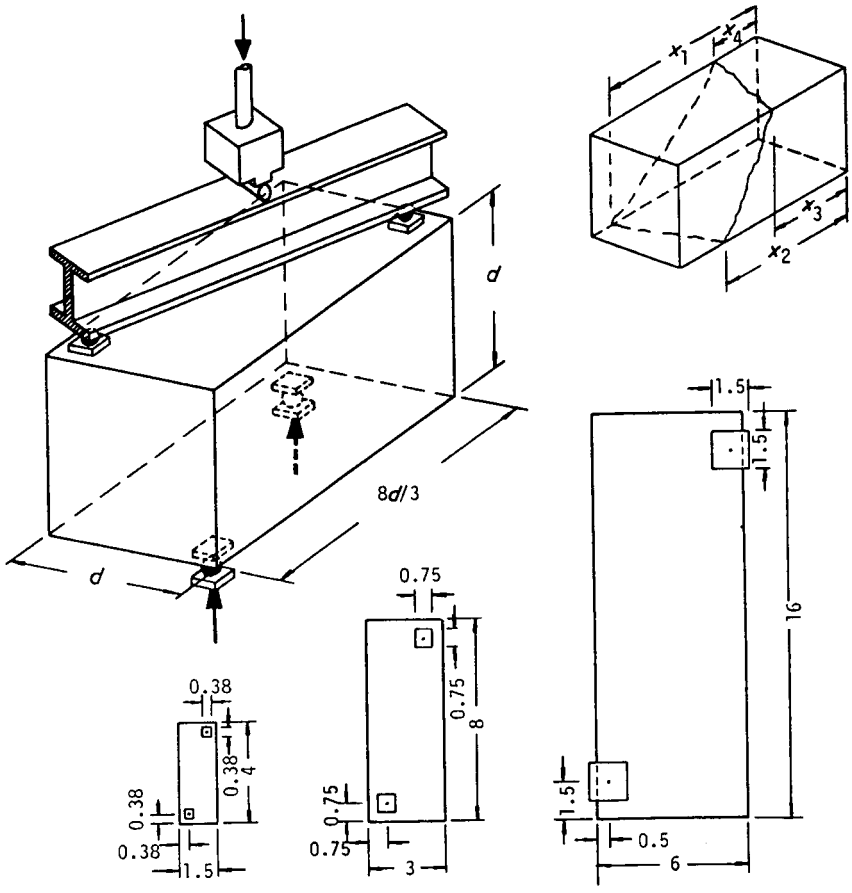

Fig. 1 Geometry of the specimens (dimensions in inches; 1 in. = 25.4 mm).

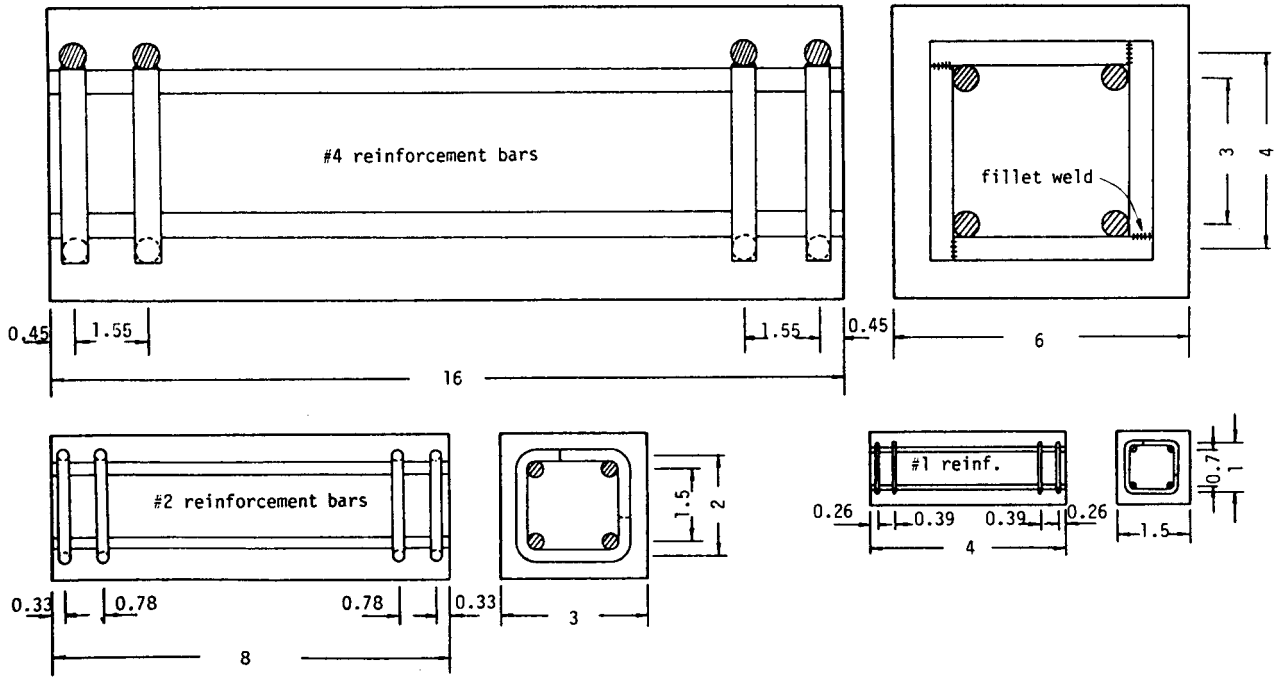

Fig. 2 Reinforcement of the specimens (dimensions in inches; 1 in. = 25.4 mm).

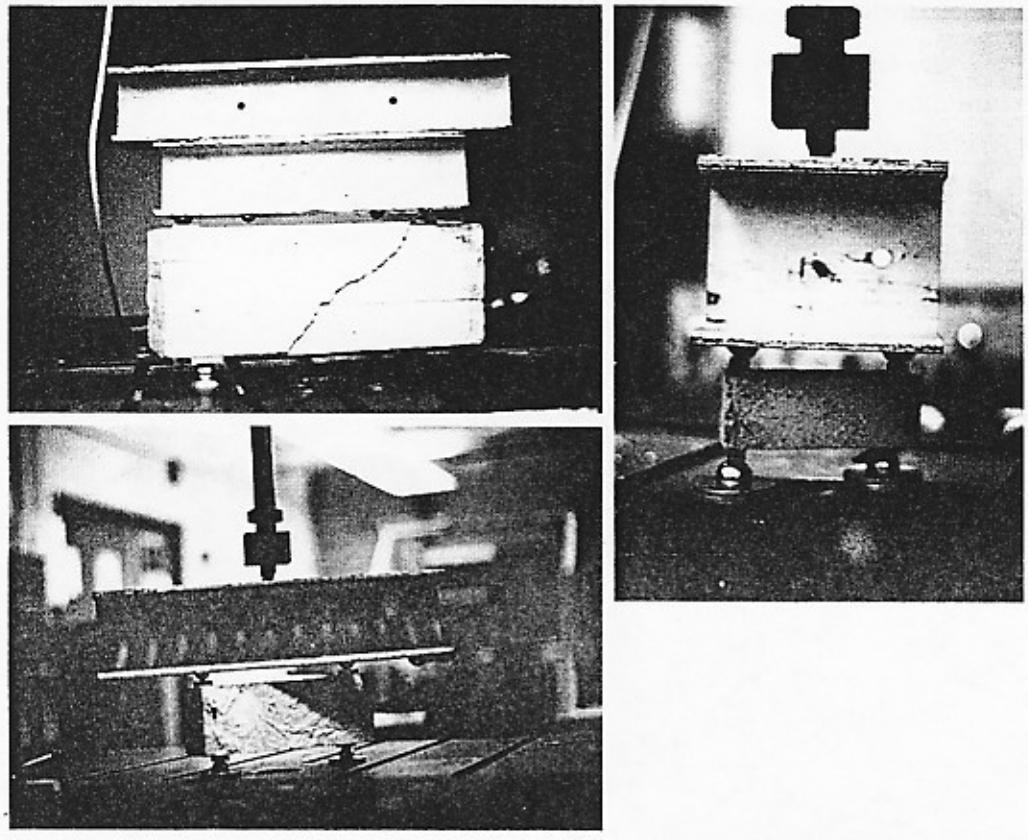

Fig. 3 Photograph of the specimens in the testing machine, showing the method of loading.

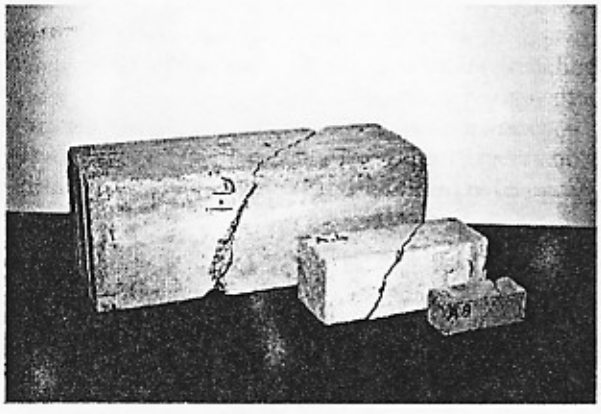

Fig. 4 Photograph of specimens of three different sizes after the test, with the shape of the cracks apparent.

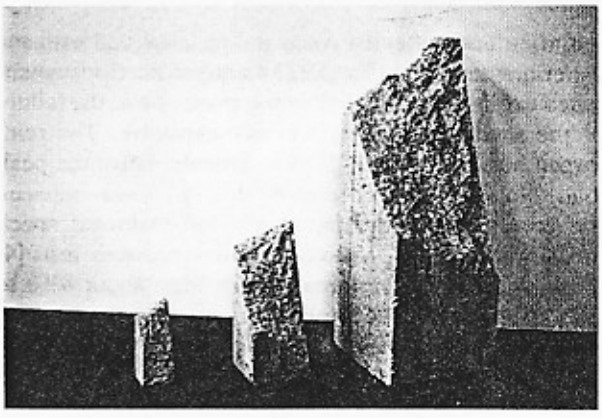

Fig. 5 Photograph of the fracture surfaces of unreinforced specimens of different sizes.

compression strengths of these specimens at age 28 days are given in Table 1.

All the specimens were tested under displacement control in a 55 tonne (120 000lb) servo-controlled closed-loop Baldwin frame modified with an MTS controller. The displacement rate was such that the maximum load was reached within about 5 min. The maximum torques measured for the individual specimens are given in Table 1 (these values include the effect of the weight of the loading beams).

All the specimens failed in the manner described in textbooks [7]. The fracture surfaces had a mean inclination of about 45° and were slightly warped on one beam side, terminating with a smaller inclination at the opposite side (see Figs 1, 3, 4 and 5). As confirmed by Table 2, the fracture surface did not simultaneously reach the reinforced segments at both specimen ends, which means that the length of the beams was apparently sufficient not to affect the maximum torque. The unreinforced beams became unstable right after crack

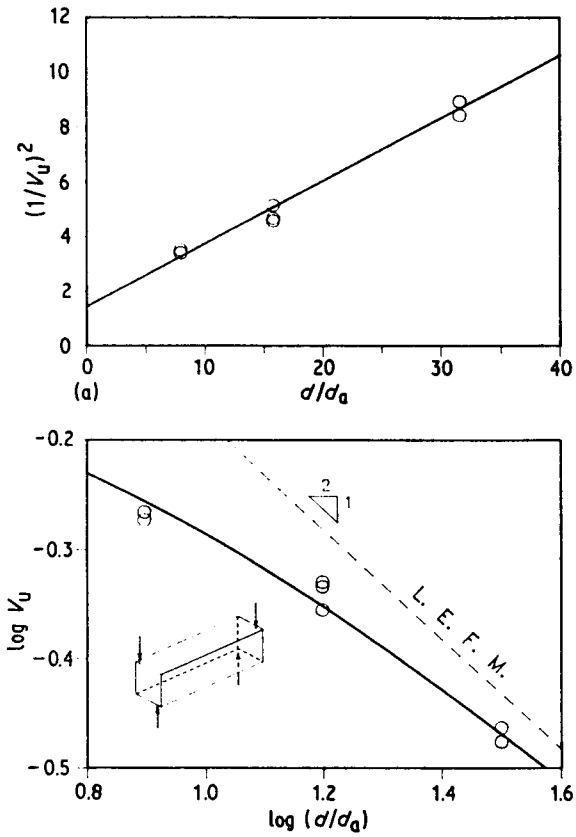

Fig. 6 Plots of the nominal stresses at failure measured on plain beams. (a) Linear plot $Y = AX + C$: $A = 0.2288$, $C = 1.4503$, $\omega_{Y|X} = 0.0440$, $r = 0.9922$. (b) Logarithmic plot: $C_1 = 0.830$, $\lambda_0 = 6.339$.

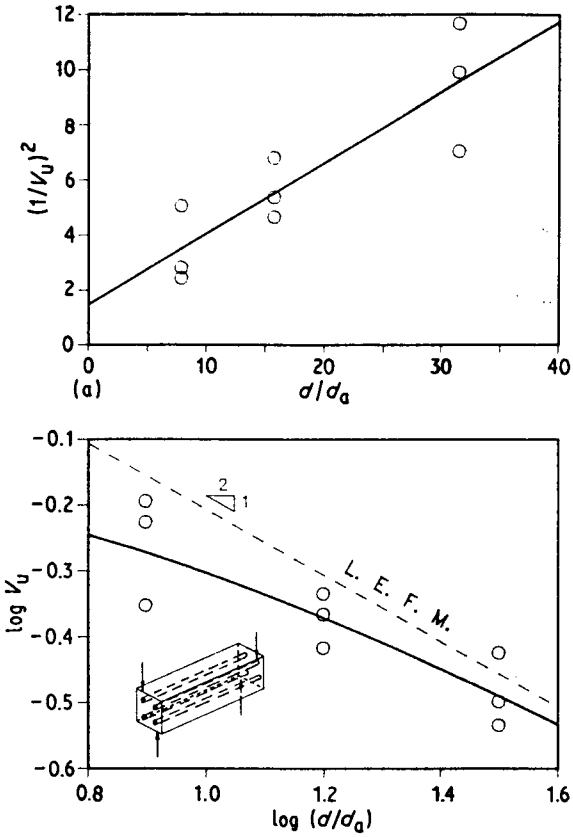

Fig. 7 Plots of the nominal stresses at failure measured on longitudinally reinforced beams. (a) Linear plot $Y = AX + C$: $A = 0.2561$, $C = 1.4798$, $\omega_{Y|X} = 0.1974$, $r = 0.8761$. (b) Logarithmic plot: $C_1 = 0.822$, $\lambda_0 = 5.778$.

initiation and softening could not be observed with the experimental set-up. The largest unreinforced specimens failed explosively, with a crushing noise, while the failure of the smaller specimens was non-explosive. The reinforced beams exhibited gradual softening after the peak load. No significant difference in failure loads between the corresponding reinforced and unreinforced specimens was recorded, although in some previous tests [4] the longitudinally reinforced beams were about 10% to 15% stronger than the unreinforced ones.

The data in Table 2 are not used in this paper but could be used as checks for finite-element simulations of the tests.

3. ANALYSIS OF TEST RESULTS

The nominal stress at failure (ultimate torsional shear stress) is usually defined as $v_u = T/\alpha d^3$ where T = maximum torque, d = the side of the square cross-section and $\alpha = 1/3$ [7]. If the failure is purely brittle and is due to distributed cracking, the nominal shear stress at failure should depend on the beam size d, and according to Bažant's size-effect law [8,9] one may expect as an approximation

$$v_u = C_1 \left(1 + \frac{d}{\lambda_0 d_a}\right)^{-1/2} \qquad (1)$$

in which d_a is the maximum aggregate size, f'_c is the standard cylindrical strength and C_1 and λ_0 are empirical coefficients (we may expect $C_1 = k_1 (f'_c)^{1/2}$ where k_1 = constant). For the dependence of C_1 on the cross section shape (see [2]). Equation 1 can be algebraically rearranged to the linear equation $Y = AX + C$ in which

$$X = \frac{d}{d_a} \qquad Y = \frac{1}{v_u^2} \qquad C = \frac{1}{C_1^2} \qquad A = \frac{C}{\lambda_0} \qquad (2)$$

This means that the test results should ideally yield a straight-line plot in the graph of Y against X. In reality there is scatter, and by linear regression one can determine the slope A of the regression line and the Y-intercept C, from which one can then easily evaluate the empirical constants C_1 and λ_0.

The results of the present tests are plotted for the plain beams in Fig. 6 and for the reinforced beams in Fig. 7. Figs 6a and 7a show linear regression plots and Figs 6b and 7b show the size-effect plots in logarithmic scales. The inclined dashed lines of slope $-1/2$ represent the size effect according to linear elastic fracture mechanics. Theoretically, this slope cannot be exceeded; it represents the strongest possible size effect in brittle failures. The curves in Figs 6b and 7b represent the optimum fit by the size-effect law in Equation 1. Figs 6a and 7a also yield

Table 1 Test results*

Plain beams				Reinforced beams			
Beam No.	d (in.)	f'_c (psi)	T (kip in.)	Beam No.	d (in.)	f'_c (psi)	T (kip in.)
A1	6.0	6325	24.09	B1	6.0	6250	21.08
A2	6.0	6325	24.80	B2	6.0	6250	22.88
A3	6.0	6400	24.08	B3	6.0	6400	27.13
A4	3.0	6325	4.21	B4	3.0	6250	3.45
A5	3.0	6325	3.97	B5	3.0	6250	3.88
A6	3.0	6400	4.17	B6	3.0	6400	4.17
A7	1.5	6325	0.61	B7	1.5	6250	0.50
A8	1.5	6325	0.60	B8	1.5	6400	0.72
A9	1.5	6325	0.61	B9	1.5	6400	0.67

* 1 in. = 25.4 mm, 1 psi = 6895 Pa, 1 kip in. = 0.1130 MN m.
f'_c is from companion cylinders.

Table 2 Failure surface (Fig. 1 top right)*

Plain beams					Reinforced beams				
Beam No.	x_1	x_2	x_3	x_4	Beam No.	x_1	x_2	x_3	x_4
A1	16.4	12.0	7.5	5.0	B1	14.5	8.4	3.0	2.5
A2	13.5	9.5	6.0	4.0	B2	14.0	12.2	5.8	0.8
A3	14.5	12.5	6.5	3.3	B3	14.0	13.0	6.5	2.5
A4	7.2	6.4	3.4	2.0	B4	6.3	3.0	2.7	0.0
A5	7.1	6.0	2.6	0.2	B5	7.2	5.0	2.6	2.8
A6	6.9	6.1	4.0	3.2	B6	7.2	5.0	2.0	0.0
A7	3.6	3.0	2.2	1.3	B7	3.2	2.1	1.5	0.5
A8	3.6	3.6	2.3	1.5	B8	3.5	2.4	1.7	0.0
A9	3.3	2.2	1.2	0.5	B9	3.3	2.3	0.3	0.5

* Measurements in inches (1 in. = 25.4 mm).

linear regression statistics from the results: $\omega_{Y|X}$, the coefficient of variation of vertical deviations from the regression line in the regression plot and r, the correlation coefficient.

The size-effect law according to Equation 1 can be introduced into the code formula based on limit analysis. Discussion of this aspect is omitted because it has already been published by Bažant and Şener [2].

One obvious limitation of the present tests is the size range. Tests on normal aggregate concrete and normal-size beams will have to be conducted to ascertain whether a revision of the code formula is indeed warranted. Nevertheless, some indication of this already exists. The existing torsional test data for larger beams [2], even though rather scattered and contaminated by the variation of factors other than the size, do also indicate a size effect consistent with Equation 1.

It is noteworthy that the reinforced beams show a similar size effect to the unreinforced ones. This observation appears to confirm the code approach which assumes, on the basis of previous tests [7], that longitudinal bars have no effect on the failure load [4]. This is despite the fact that failure of the reinforced beams involves not only the propagation of a fracture surface through the concrete but also a loss of bonding of the steel bars. The explanation may be that bonding is lost before the maximum load is reached, rather than simultaneously with the failure at maximum load.

4. CONCLUSIONS

1. In agreement with the analysis of some previous test data [2], the test results confirm the existence of a significant size effect. This suggests that the existing design code formulae, which exhibit no size effect, should be improved.

2. As far as the scatter of the results permits it to be seen, the test results are consistent with Bažant's size effect law (Equation 1). However, due to the scatter as well as the limited size range and limited scope, the results cannot be interpreted as a proof of applicability of this law. That this law should be applicable rests solely on the

perception that the cause of the size effect is principally of fracture-mechanics type (rather than, for example, of a statistical nature).

3. Although the scatter for the reinforced beams tested was larger than for the unreinforced ones, it nevertheless appears that the size effect is equally strong for the plain and the reinforced beams. Moreover, the parameter λ_0, which characterizes the centre of the transition between the strength failure criterion and the fracture mechanics failure criterion [8], is about the same for the plain and reinforced beams; approximately $\lambda_0 = 6$.

4. The test results confirm that longitudinal bars make no significant contribution to the torsional strength.

ACKNOWLEDGEMENTS

The experiments were partially supported under a co-operative project with Universidad Politecnica de Madrid under the US–Spanish Treaty (Grant CCA-830971 to Northwestern University). The theoretical work on the size effect, underlying the present formulation, was supported under AFOSR Grant No. 83-0009 to Northwestern University, monitored by Dr Spencer T. Wu.

REFERENCES

1. ACI Standard, 'Commentary on Building Code Requirements for Reinforced Concrete,' ACI 318M-83J (ACI, Detroit, 1984).
2. Bažant, Z. P. and Şener, S., 'Size effect in torsional failure of concrete beams,' *J. Struct. Engng, Proc. ASCE* **113** (1987) 2125–2136.
3. Hsu, T. T. C., 'Torsion of structural concrete – plain concrete rectangular sections, in 'Torsion of Structural concrete', SP-18 (American Concrete Institute, Detroit, 1968) pp. 203–238.
4. *Idem*, 'Torsion of Reinforced Concrete' (Van Nostrand Reinhold, New York, 1984).
5. Humphreys, R., 'Torsional properties of prestressed concrete,' *Struct. Engnr* **35** (6) (1957) 213–224.
6. McMullen, A. E. and Daniel, H. R., 'Torsional strength of longitudinally reinforced beams containing an opening,' *ACI J.* **72** (8) (1975) 415–420.
7. Park, P. and Paulay, T., 'Reinforced Concrete Structures,' (Wiley, New York, 1975).
8. Bažant, Z. P., 'Size effect in blunt fracture: concrete, rock, metal,' *J. Engng Mech., Proc. ASCE* **110** (1984) 518–535.
9. *Idem*, 'Mechanics of fracture and progressive cracking in concrete structures,' in 'Fracture Mechanics Applied to Engineering Problems,' edited by G. C. Sih (Nijhoff, The Hague, 1985) pp. 1–94.